Research Article Vol. 2, No. 3 / 15 March 2019 / OSA Continuum 973

PAM4 transmission over 360 km of fibre using optical phase conjugation

K. R. H. Bottrill,* N. Taengnoi, F. Parmigiani, D. J. Richardson, and P. Petropoulos

Optoelectronics Research Centre, University of Southampton, Southampton, SO17 1BJ, UK
krhb1g12@soton.ac.uk

Abstract: We demonstrate the transmission of 3×20 Gbaud PAM4 signals over a 360 km, field-deployed, amplified transmission link. We compare dispersion compensation using optical phase conjugation (OPC) to dispersion compensating fibre (DCF) and find an improvement in the received bit error ratio of an order of magnitude using our OPC implementation.

1. Introduction

The continued growth in high bandwidth content sharing, notably over-the-top video services, place particular pressure on metro networks with caching increasingly being used to realise bandwidth savings in core networks [1]. As such, transmission technologies which can deliver the required data rate as well as the necessary interface density in a cost-effective way are highly sought-after. Whilst coherent optical transmission offers undeniable benefits in terms of receiver sensitivity, enabling longer reaches and higher spectral efficiencies than its direct-detection counterpart, the latter has so far retained favour in many settings owing to its simplicity and affordability. Direct-detection formats in general benefit from reduced hardware requirements compared to coherent formats - modulation can be performed with simple Mach-Zehnder modulators (MZMs) [2], electro-absorption modulators [3,4] or even directly modulated lasers [5], whilst detection can be performed with single photodetectors, requiring no local optical oscillators and in many cases, relatively simple digital signal processing (DSP) requirements. PAM4 is just such a format and is notable for its particularly simple implementation and low DSP requirements leading to low power consumption relative to other direct-detection formats, such as carrier amplitude and phase modulation (CAP) and discrete multi-tone (DMT) [6,7]. Of late, PAM4 has seen rapid adoption in datacentres, featuring in a number of short-reach 100G extensions as well as many initial 200G and 400G extensions to the 802.3 ethernet standard. Improving the reach of PAM4 transmissions further would allow these cost-saving benefits to be extended to regional- and core- metro networks as well as interconnects between more dispersed data-centres [7,8].

We focus on solutions for extending the reach of PAM4 transmission in the C-band. Assuming transmission over dispersive fibre, such as SMF28, with increasing transmission distance comes increasing distortion due to chromatic dispersion [7,9,10], which at some point will require some means of mitigation if an acceptable signal quality is to be maintained. Dispersion compensating fibre (DCF) is a natural first approach to solving this issue, and has been used to demonstrate transmission of 3×28 Gbaud PAM4 signals over 100 km [11]. DCF, however, is far from ideal, notably increasing the loss of a link by a factor of approximately 1.5 (owing to DCF's attenuation of $0.5\,\mathrm{dB.km^{-1}}$ compared to the $0.18\,\mathrm{dB.km^{-1}}$ of SMF28 in the C-band) and increasing polarisation mode dispersion (PMD) of the link. Latency is also a particularly important consideration for datacentre interconnects, often determining the location and population of

#346409 https://doi.org/10.1364/OSAC.2.000973
Journal © 2019 Received 21 Sep 2018; revised 14 Dec 2018; accepted 18 Dec 2018; published 13 Mar 2019

OSA CONTINUUM

datacentres providing services to large metropolitan areas, and with typical DCFs possessing a chromatic dispersion of $\approx -100\,\mathrm{ps.nm^{-1}.km^{-1}}$ [12], compared to SMF28's $17\,\mathrm{ps.nm^{-1}.km^{-1}}$, the use of DCFs for dispersion compensation typically represents an increase in latency of about $\frac{17}{100} = 17\%$ (assuming a similar transmission speed in both DCF and SMF). Fibre Bragg gratings (FBG) might be considered to be an upgrade over DCFs, offering a comparatively much lower loss as well as reduced nonlinearity[13] and much lower latency, however, the most cost-effective FBG solutions, single-channel dispersion compensators, compromise the colorless nature of transceivers. Dispersion compensation through predistortion at the transmitter using directly modulated lasers has also been demonstrated (for example in [14]), and these approaches offer a promising solution to dispersion compensation without incurring changes to the transmission link. DSP based chromatic dispersion mitigation techniques suitable for direct-detection formats have been demonstrated, such as maximum likelihood sequence estimation (MLSE) [15–17], and Kramers-Kronig detection [18–20]. MLSE has been demonstrated for reach extension of approximately 60 km of SMF28 in OOK demonstrations [16,17] and transmission of 23 GBd PAM4 over 23 km of SMF28. It has later been combined with pulse chirping using a dual-drive MZM and a feed-forward equaliser to demonstrate 64 GBd PAM4 transmission [21] over 80 km. Kramers-Kronig receivers are a relatively recent development, first discussed for use in fibre optic transmission systems in 2016 [20], which allow a single photodetector to be used for measurement of a signal's amplitude and phase, provided that the minimum phase condition is satisfied. Kramers-Kronig reception does come at the price of additional complexity, however, knowledge of a signal's amplitude and phase allows for full chromatic dispersion post-compensation to be implemented digitally, albeit with a penalty in BER compared to optical compensation or full coherent detection [20].

In this paper, we demonstrate dispersion compensation of PAM4 signals using mid-link optical phase conjugation (OPC) [22–24], also known as mid-span spectral inversion. OPC is characterised by its format and baudrate agnosticism, potential for nonlinear compensation and naturally multi-channel operation. Note, that whilst OPC has of late been demonstrated for compensation of nonlinearities in long-haul transmission [25–28], we deploy it here strictly for dispersion compensation. For optimal dispersion compensation, a requirement of OPC is its need to be deployed at the exact mid-point of a link, access to which we had in our transmission link. We expect some tolerance to span length mismatch can be conveniently provided by DSP techniques discussed above, such as MLSE detection. The aim of this study is to demonstrate what performance characteristics can be expected from an OPC equipped link carrying PAM4. For context, we compare the performance of the system to an equivalent DCF equipped reference link and show improved performance using OPC due to a combination of reduced link loss as well as reduced nonlinear and PMD impairments from the removal of the DCF modules. We demonstrate our scheme upon a WDM band containing 3×20 Gbaud PAM4 signals and show an improvement in BER by an order of magnitude across all signals when they are transmitted over a field-deployed link totalling 360km in length.

2. Experimental setup

A schematic of the experimental set-up for the study is provided in Fig. 1, separated into the following sub-systems: a) the transmitter, b) the receiver, c) the OPC device itself, d) link set-up with dispersion compensation performed using DCMs, and e) link set-up with dispersion compensation performed using OPC.

The transmitter, shown in Fig. 1-a, consists of three independent CW lasers with frequencies 195.05 THz (1537.00 nm), 195.10 THz (1536.61 nm) and 195.15 THz (1536.22 nm), in this document referred to as Ch50.5, Ch51.0 and Ch51.5, respectively, multiplexed so that they can be modulated in the same device. This device is a dual-drive Mach-Zehnder modulator with each arm driven by the same 4-level electrical waveform but with opposite polarity, resulting in 20 GBaud

OSA CONTINUUM

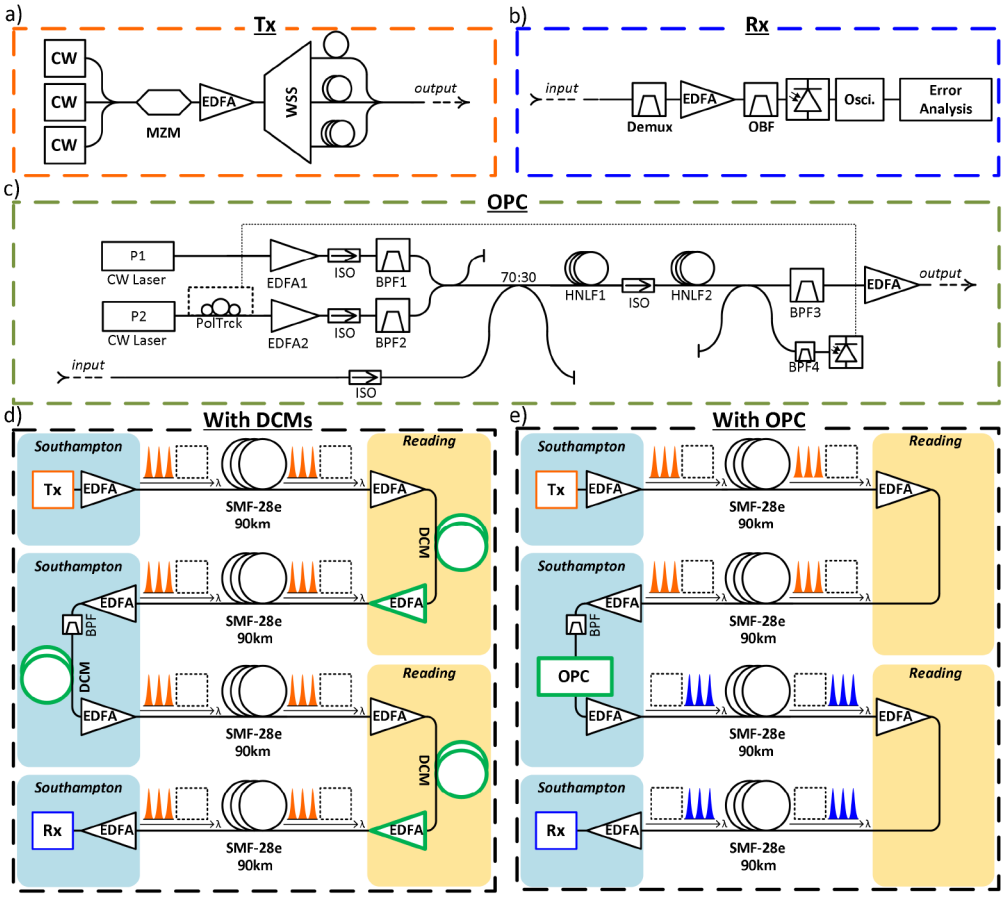

Fig. 1. a) Transmitter, b) Receiver, c) OPC set-up d) link configuration using DCF for dispersion compensation and e) link configuration using OPC for dispersion compensation.

optical PAM4 signals. After modulation, the signals are decorrelated by demultiplexing them using a programmable optical filter, propagating them along patchcords of suitably different length, before finally recombining them using an optical coupler. An EDFA is used to raise the signal band's power to a fixed total power of 13 dBm before the programmable filter in order to reduce the effects of loss of this process.

PAM4, being a direct-detection format, requires only a simple receiver. Figure 1-b shows the set-up of the receiver, the hardware of which consists of a demultiplexing filter, an EDFA and a noise rejection filter to facilitate BER measurements, and finally a photodetector whose output drives an 80 GSa.s^{-1} real-time oscilloscope. The decoding software consists of a simple histogram based thresholding algorithm [29] followed by a software implementation of edge-detection based clock recovery [30].

The OPC device itself, shown in Fig. 1-c, utilised an orthogonally pumped FWM scheme in order to provide polarisation independent conjugation of the signal band [27]. Two pump lasers, located at 194.5 THz (1541.45 nm) and 195.3 THz (1535.04 nm), were each passed through high power EDFAs. These two pumps were then passed through optical bandpass filters with full-width at half maximum of 0.3 nm to reduce out-of-band amplified spontaneous emission (ASE), before they were combined using a 3 dB coupler, one output of which was discarded whilst the other was combined with the signal band to be conjugated using a 30:70 coupler biased towards the

OSA CONTINUUM

pumps. With the signal band and pumps combined, they could then be propagated through the nonlinear element to undergo FWM. The nonlinear element consisted of a pair of strained, Germanium doped, dispersion flattened HNLFs, the first of length 100 m and the second 160 m, connected by an optical isolator to increase the Brillouin threshold of the fibre cascade [31]. The Brillouin threshold of the aggregate was found to be approximately 25.5 dBm, and so a power of 25 dBm per pump was used for conjugation. The zero dispersion wavelength of both fibres was 1530 nm, and the desire to achieve good conversion efficiency in the fibre governed our decision to locate the system about the low-wavelength end of the C-band. After the signal band and pumps passed through the HNLF cascade, the phase conjugated idlers were isolated using an optical bandpass filter before they were amplified to 8dBm using an EDFA. In order to obtain polarisation independent generation of the conjugate idlers, it is known that in a isotropic fibre, the two pumps must possess an orthogonal polarisation relative to each other [32,33]. To achieve this state we used a polarisation tracker inline with one of the pumps at the beginning of the system. We extracted one of the first order tones generated from the degenerate FWM interaction between the two pumps and provided this as an error signal to the polarisation tracker whose action was to search for a polarisation minimising the power of this tone. In the ideal case, when this tone is minimised, the pumps are orthogonal. Figure 2 shows the spectrum after propagation through the HNLF, with pumps, signals and idlers labelled, and indicates a parametric conversion efficiency of ≈ -2 dB. It can be seen that the conjugated idlers generated by the FWM process possess a similar power flatness to the signals originally launched into the device.

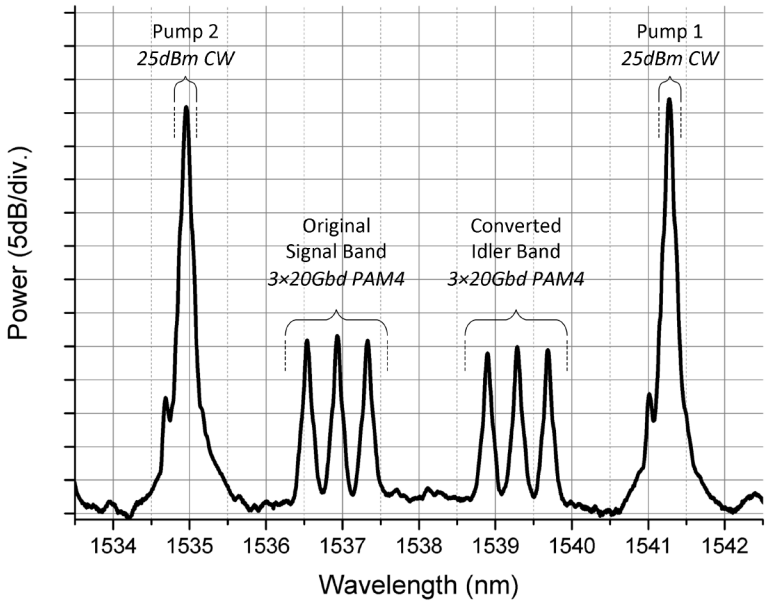

Fig. 2. Spectrum after propagation through HNLF.

Two pairs of fibre of the national dark fibre infrastructure service (NDFIS), UK, were used to realise a link with a total transmission distance of 360km of G.652d compliant fibre. The link consisted of two round trips from Southampton to Reading, two cities in the south of England, resulting in fibre spans of 90 km in length, such that the beginning, middle and end of the link all lay geographically at Southampton. When using either DCMs or OPC for dispersion compensation, each SMF span was followed by an EDFA with gain equal to the loss of the section preceding it, as shown in Figs. 1-d and -e. In both cases, an optical bandpass filter was incorporated in the middle of the link to reject the ASE surrounding the signals. This filter

OSA CONTINUUM

was included in both cases so that the DCM scenario could benefit from this mid-link ASE rejection, and so that it could be proven that the signal band truly benefits from the conjugation operation, and not simply mid-link filtering. Figure 1-d shows the location of the DCM modules in the DCM equipped link; one module for each trip to Reading (each followed by an EDFA to compensate for the loss of the DCMs themselves) and one module in the middle of the link (which lies at Southampton). In contrast, when dispersion compensation was performed by OPC, we simply installed the OPC device in the middle of the link with no further modifications. It is important to note that, due to the mechanism of action of dispersion compensation using OPC, it is only necessary that the chromatic dispersion before and after the point of conjugation is equal. Provided this requirement is met, the link may be extended without the addition of any other elements. The same cannot be said for the DCM approach, wherein an extension of the link must be associated with the addition of further DCM modules, increasing link loss as well as latency beyond that incurred by the additional transmission fibre. Naturally, as the conjugated band lay at a different wavelength compared to the original signal band, in the OPC case, the data were detected at different carrier wavelengths compared to the original transmission.

3. Results

As the inclusion of DCMs or OPC in the link transforms the nonlinear characteristics of the link, we chose to characterise all scenarios by measuring the BER of the signals after transmission for a range of span launch powers (defined as the total optical power entering each span of SMF).

As expected, the system performance with the OPC included was highly dependent upon the power with which the signal band was launched into the HNLF of the OPC [34], which we shall refer to as the OPC launch power. This effect was studied for a single channel case by deactivating all signals other than CH51.5. The signal power launched into the OPC was varied and the best achievable BER was found for each case by varying the span launch power. In other words, for each point plotted in Fig. 3-a, a range of span launch powers was also tested to determine the best achievable BER for each OPC launch power. The results of this measurement are provided in

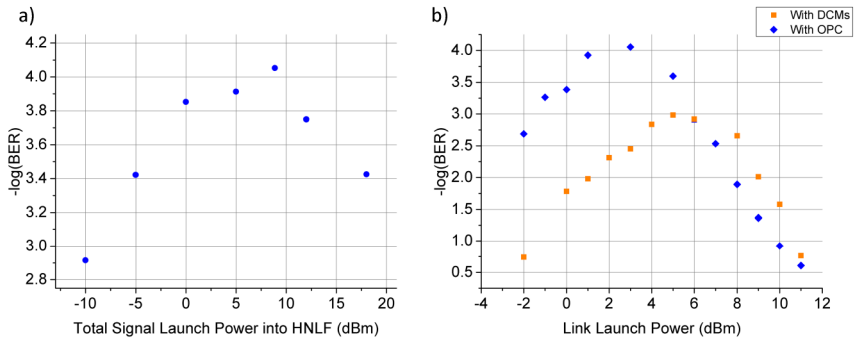

Fig. 3. For the single channel case: a) BER vs launch power into HNLF, b) BER vs link launch power.

Fig. 3-a. As can be expected, we were able to identify an optimal OPC launch power, 9 dBm, for the single channel case, resulting in a BER of 8.9×10^{-5}. The low power edge of the curve suffers a reduced BER relative to the peak due to linear noise effects (the converted idler must compete with the ASE floor in the HNLF accompanying the pumps), whilst the high power edge suffers a reduced BER due to nonlinear effects (predominantly SPM) that the signal experiences during its propagation in the HNLF. The optimum can be seen to occur for a certain trade-off between these two effects. Figure 3-b provides the curves traced by varying the span launch power, both for the DCM equipped link and for the OPC equipped link (using the optimal OPC

OSA CONTINUUM

launch power of 9 dBm). In this case, we can see that the optimal BER of the OPC equipped link of 8.9×10^{-5} (occurring for a span launch power of 3 dBm) exceeds the BER of 1×10^{-3} for the DCM equipped case (occurring for a span launch power of 5 dBm) by a large margin. It is interesting to note that the optimal span launch power for the OPC equipped link is 2 dB lower than for the DCM equipped link, contrary to what might be expected, as the use of OPC is often associated with a reduction of nonlinear impairments in the link. The reason for this shift is nonlinear noise loading of the signal during phase conjugation, which essentially accelerates the onset of nonlinear degradation upon further transmission.

To support this conclusion, we modelled both the DCM equipped and OPC equipped links using the commercial simulation software VPIphotonics Design Suite and collected the results provided in Fig. 4 when using the nominal fibre lengths and parameters used in the experimental system. Figure 4-a provides a plot showing how the peak BER for each link varies with the noise figure of the EDFAs used in the link. As can be seen, the quality of the DCM equipped link (orange squares) is affected by an increasing noise figure more severely than the OPC equipped link (blue diamonds). This is to be expected, because, as can be seen in Fig. 1, the OPC equipped link has fewer EDFAs than the DCM equipped link. Figure 4-b shows how the link launch power required for optimum BER varies with the power with which the signal is launched into the HNLF during phase conjugation (blue diamonds). For reference, a dashed orange line showing the optimum link launch power for the simulated DCM equipped link is provided, which, naturally, does not depend upon the launch power into the HNLF. The plot shows that for lower signal launch powers, the optimum link power occurs at higher powers than for the DCM equipped link. Increasing the signal power launched into the HNLF does, however, result in the optimum launch power decreasing, eventually to the point where it occurs at lower powers than that for the DCM-equipped link, just as witnessed in Fig. 3.

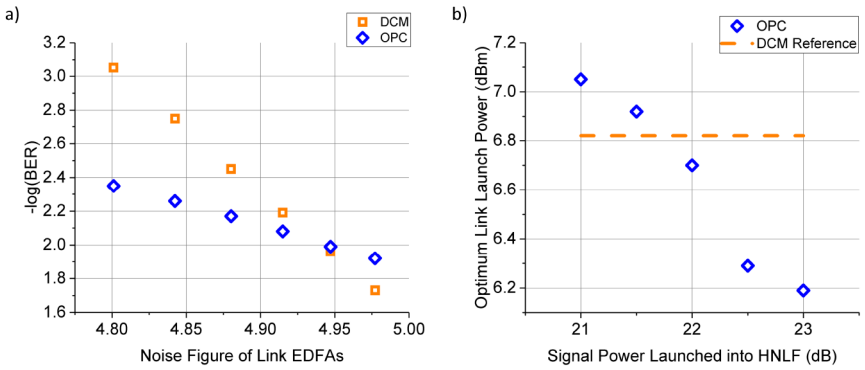

Fig. 4. Results on simulations with VPIphotonics Design Suite a) BER as it varies with the Noise Figure of the EDFAs in the link for both DCM equipped link (orange squares) and OPC equipped link (blue diamonds), b) optimum link launch power as it varies with signal power launched into HNLF (blue diamonds), DCM reference (orange dashed line).

For the 3 channel case, it was found that the optimal total power with which to launch the signals into the HNLF was 3 dBm. This reduced optimal power relative to the single channel case can be understood to be due to the increased nonlinear penalties experienced by the signals due to XPM and FWM between them which was absent in the single channel case. These effects can be quite strong, given that the system is essentially optimised for FWM through the use of a low dispersion, highly nonlinear fibre. We have included simulations of a simple wavelength conversion process (without transmission through fibre, i.e. wavelength conversion directly after the transmitter and directly before the receiver) below using VPIphotonics (Fig. 5), which shows a decrease in optimal per channel launch power of 9.79dB, showing the scale of the difference

OSA CONTINUUM

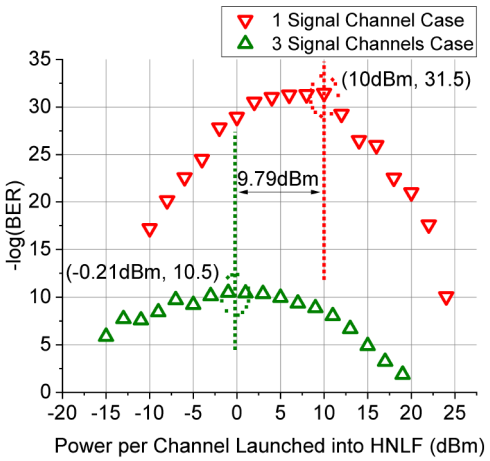

Fig. 5. Simple wavelength conversion simulation showing the change in peak power which can possibly be observed when moving from a 1 channel to a 3 channel converted band. Optimal launch powers are identified with dashed lines.

between the single channel case (red, downward pointing triangles) and the three channel case (green, upward pointing triangles) which can be observed in such systems and comparable to what we observe in our experiment. Note that the observable difference is heavily dependent upon many parameters of the system - the pump power, dispersion of fibre, PMD etc.

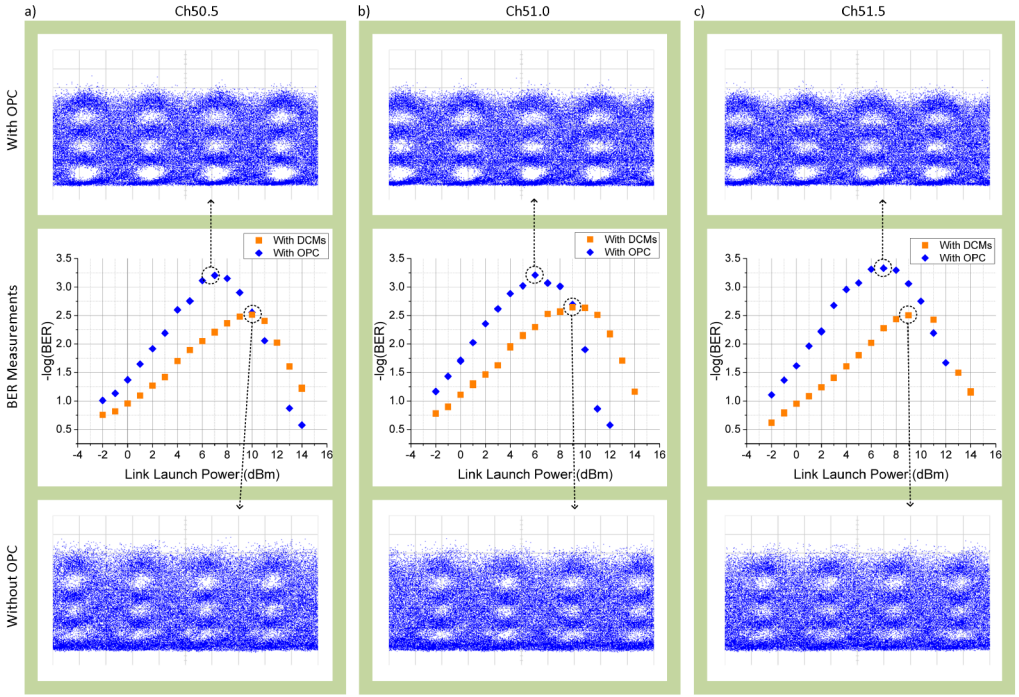

Fig. 6. For the three channel case, eye diagrams and BER vs link power curves for: a) Ch50.5, b) Ch51.0 and c) Ch51.5.

OSA CONTINUUM

Figure 6 contains BER plots for each channel in the 3 channel case for both the OPC equipped link and the DCM equipped link. It can be seen that, with the DCMs in place, all three channels obtain a minimum BER of 3×10^{-3} for span launch powers around 9 dBm, whilst in the OPC case, all three signals obtain BERs of about 6×10^{-4} or better, for span launch powers of 7 dBm. Again, we see that the optimum launch power for the OPC is lower, in this case 3 dB lower than the DCM equipped link, which can once again be explained by nonlinear noise accrued during the phase conjugation process. Means of reducing this effect include increasing the pump power in the fibre in order to reduce the required signal launch powers into the HNLF and reducing the ASE floor with which the idlers have to compete through better filtering of the pumps and signals. Eye diagrams are also provided for the optimum launch power in each curve in Fig. 6, where it can be seen that in all cases, the eye diagrams obtained for the OPC equipped link are clearly visually better than those in the DCM equipped link. Interestingly, we can see that for the OPC equipped link, the uppermost eye is notably more deteriorated than the lowest eye, which can again be explained due to nonlinear noise acquired during the phase conjugation process.

4. Conclusions

With chromatic dispersion identified as the first hurdle to be overcome when extending the reach of PAM4 transmissions, we proposed that dispersion compensation via OPC could offer benefits over dispersion compensation via DCMs in terms of OSNR and latency. We demonstrated this principle by transmitting 3×20 GBaud PAM4 signals over a total distance of 360km across a field-deployed optical fibre network. The use of OPC for dispersion compensation allowed us to obtain BERs of 6×10^{-4} versus 3×10^{-3} for the DCM equipped case. These improvements are expected to increase as reach is extended further.

Funding

Engineering and Physical Sciences Research Council (EPSRC) (NS/A000021/1, S002871/1).

Acknowledgments

The data for this work is accessible through the University of Southampton Institutional Research Repository (DOI:10.5258/SOTON/D0501) [35]. This experiment was performed upon the jointly EPSRC/JISC-supported National Dark Fibre Infrastructure Service (NDFIS), UK. This work was supported by the UK EPSRC grant EP/S002871/1 as part of the Photonic Phase Conjugation Systems (PHOS) project. We gratefully acknowledge the support of NVIDIA Corporation for the provision of a Titan Xp GPU used in the numerical work.

References

1. Bell Labs, "Metro Network Traffic Growth: An Architecture Impact Study Strategic White Paper," Tech. Rep. (2013).
2. S. Shao, J. Ding, L. Zheng, K. Zou, L. Zhang, F. Zhang, and L. Yang, "Optical PAM-4 Signal Generation using a Silicon Mach-Zehnder Optical Modulator," Opt. Express **25**(19), 23003–23013 (2017).
3. X. Xu, E. Zhou, G. N. Liu, T. Zuo, Q. Zhong, L. Zhang, Y. Bao, X. Zhang, J. Li, and Z. Li, "Advanced Modulation Formats for 400-Gbps Short-reach Optical Inter-connection," Opt. Express **23**(1), 492–500 (2015).
4. U. Troppenz, M. Narodovitch, C. Kottke, G. Przyrembel, W. D. Molzow, A. Sigmund, H. G. Bach, and M. Moehrle, "1.3 μm Electroabsorption Modulated lasers for PAM4/PAM8 single channel 100 Gb/s," in *26th International Conference on Indium Phosphide and Related Materials (IPRM)* (2014), pp. 1–2.
5. P. P. Baveja, M. Li, D. Wang, C. Hsieh, H. Zhang, N. Ma, Y. Wang, J. Lii, Y. Liang, C. Wang, I. L. Ho, and J. Zheng, "56 Gb/s PAM-4 Directly Modulated Laser for 200G/400G Data-center Optical Links," in *2017 Optical Fiber Communications Conference and Exhibition (OFC)* (2017), pp. 1–3.
6. J. L. Wei, J. D. Ingham, D. G. Cunningham, R. V. Penty, and I. H. White, "Performance and Power Dissipation Comparisons Between 28 Gb/s NRZ, PAM, CAP and Optical OFDM Systems for Data Communication Applications," J. Lightwave Technol. **30**(20), 3273–3280 (2012).
7. A. Dochhan, H. Griesser, N. Eiselt, M. H. Eiselt, and J. P. Elbers, "Solutions for 80 km DWDM Systems," J. Lightwave Technol. **34**(2), 491–499 (2016).

OSA CONTINUUM

8. B. Teipen, N. Eiselt, A. Dochhan, H. Griesser, M. Eiselt, and J. P. Elbers, "Investigation of PAM-4 for Extending Reach in Data Center Interconnect Applications," in *2015 17th International Conference on Transparent Optical Networks (ICTON)* (2015), pp. 1–4.
9. R. C. Figueiredo, A. L. N. Souza, S. M. Ranzini, A. Chiuchiarelli, L. H. H. Carvalho, and J. D. Reis, "Investigation of 56-GBd PAM4 Bandwidth and Chromatic Dispersion Limitations for Data Center Applications," in *2017 SBMO/IEEE MTT-S International Microwave and Optoelectronics Conference (IMOC)* (2017), pp. 1–5.
10. T. Yoshimatsu, M. Nada, S. Kanazawa, F. Nakajima, H. Matsuzaki, and K. Sano, "Dispersion Tolerance of 100-Gbit/s PAM4 Optical Link Utilizing High-Speed Avalanche Photodiode Receiver," IEICE Electron. Express **15**(16), 20180624 (2018).
11. S. Yin, T. Chan, and W. I. Way, "100-km DWDM Transmission of 56-Gb/s PAM4 per λ via Tunable Laser and 10-Gb/s InP MZM," IEEE Photonics Technol. Lett. **27**(24), 2531–2534 (2015).
12. S. Ramachandran, *Fiber Based Dispersion Compensation* (Springer-Verlag New York, 2007).
13. G. Gnanagurunathan and F. A. Rahman, "Comparing FBG and DCF as Dispersion in the Long Haul Narrowband WDM Systems," in *2006 IFIP International Conference on Wireless and Optical Communications Networks* (2006), p. 4.
14. Z. Liu, G. Hesketh, B. Kelly, J. O'Caroll, R. Phelan, D. J. Richardson, and R. Slavík, "300-km Transmission of Dispersion Pre-compensated PAM4 Using Direct Modulation and Direct Detection," in *Optical Fiber Communication Conference* (Optical Society of America, 2017), p. Th3D.6.
15. C. Chen, X. Tang, and Z. Zhang, "Transmission of 56-Gb/s PAM-4 over 26-km Single Mode Fiber Using Maximum Likelihood Sequence Estimation," in *Optical Fiber Communication Conference* (Optical Society of America, 2015), p. Th4A.5.
16. M. S. Alfiad, D. van den Borne, F. N. Hauske, A. Napoli, A. M. J. Koonen, and H. de Waardt, "Maximum-Likelihood Sequence Estimation for Optical Phase-Shift Keyed Modulation Formats," J. Lightwave Technol. **27**(20), 4583–4594 (2009).
17. J. M. Gene, P. J. Winzer, S. Chandrasekhar, and H. Kogelnik, "Joint PMD and Chromatic Dispersion Compensation Using an MLSE," in *2006 European Conference on Optical Communications* (2006), pp. 1–2.
18. M. Zhu, J. Zhang, X. Yi, H. Ying, X. Li, M. Luo, Y. Song, X. Huang, and K. Qiu, "Optical Single Side-Band Nyquist PAM-4 Transmission using Dual-Drive MZM Modulation and Direct Detection," Opt. Express **26**(6), 6629–6638 (2018).
19. L. Shu, J. Li, Z. Wan, F. Gao, S. Fu, X. Li, Q. Yang, and K. Xu, "Single-Lane 112-Gbit/s SSB-PAM4 Transmission With Dual-Drive MZM and Kramers-Kronig Detection Over 80-km SSMF," IEEE Photonics J. **9**(6), 1–9 (2017).
20. A. Mecozzi, C. Antonelli, and M. Shtaif, "Kramers-Kronig Coherent Receiver," Optica **3**(11), 1220–1227 (2016).
21. Q. Zhang, N. Stojanovic, C. Xie, C. Prodaniuc, and P. Laskowski, "Transmission of Single Lane 128 Gbit/s PAM-4 Signals over an 80 km SSMF Link, Enabled by DDMZM Aided Dispersion Pre-Compensation," Opt. Express **24**(21), 24580–24591 (2016).
22. A. Yariv, D. Fekete, and D. M. Pepper, "Compensation for Channel Dispersion by Nonlinear Optical Phase Conjugation," Opt. Lett. **4**(2), 52–54 (1979).
23. A. Corchia, C. Antonini, A. D'Ottavi, A. Mecozzi, F. Martelli, P. Spano, G. Guekos, and R. Dall'Ara, "Mid-span Spectral Inversion without Frequency Shift for Fiber Dispersion Compensation: a System Demonstration," IEEE Photonics Technol. Lett. **11**(2), 275–277 (1999).
24. C. Lorattanasane and K. Kikuchi, "Design Theory of Long-distance Optical Transmission Systems using Midway Optical Phase Conjugation," J. Lightwave Technol. **15**(6), 948–955 (1997).
25. I. Sackey, F. D. Ros, J. K. Fischer, T. Richter, M. Jazayerifar, C. Peucheret, K. Petermann, and C. Schubert, "Kerr Nonlinearity Mitigation: Mid-Link Spectral Inversion Versus Digital Backpropagation in 5×28-GBd PDM 16-QAM Signal Transmission," J. Lightwave Technol. **33**(9), 1821–1827 (2015).
26. A. D. Ellis, M. Tan, M. A. Iqbal, M. A. Z. Al-Khateeb, V. Gordienko, G. S. Mondaca, S. Fabbri, M. F. C. Stephens, M. E. McCarthy, A. Perentos, I. D. Phillips, D. Lavery, G. Liga, R. Maher, P. Harper, N. Doran, S. K. Turitsyn, S. Sygletos, and P. Bayvel, "4 Tb/s Transmission Reach Enhancement Using 10×400 Gb/s Super-Channels and Polarization Insensitive Dual Band Optical Phase Conjugation," J. Lightwave Technol. **34**(8), 1717–1723 (2016).
27. S. Yoshima, Y. Sun, Z. Liu, K. R. H. Bottrill, F. Parmigiani, D. J. Richardson, and P. Petropoulos, "Mitigation of Nonlinear Effects on WDM QAM Signals Enabled by Optical Phase Conjugation with Efficient Bandwidth Utilization," J. Lightwave Technol. **35**(4), 971–978 (2017).
28. A. D. Ellis, M. A. Z. A. Khateeb, and M. E. McCarthy, "Impact of Optical Phase Conjugation on the Nonlinear Shannon Limit," J. Lightwave Technol. **35**(4), 792–798 (2017).
29. N. Dong-Nhat, M. A. Elsherif, and A. Malekmohammadi, "Investigations of High-Speed Optical Transmission Systems Employing Absolute Added Correlative Coding (AACC)," Opt. Fiber Technol. **30**, 23–31 (2016).
30. A. Buchwald and K. Martin, *Integrated Fiber-Optic Receivers*, The Springer International Series in Engineering and Computer Science (Springer US, 2012).
31. M. E. Marhic, *Fiber Optical Parametric Amplifiers, Oscillators and Related Devices* (Cambridge University Press, Cambridge, 2012).
32. K. K. Y. Wong, M. E. Marhic, K. Uesaka, and L. G. Kazovsky, "Polarization-independent Two-pump Fiber Optical Parametric Amplifier," IEEE Photonics Technol. Lett. **14**(7), 911–913 (2002).

OSA CONTINUUM

33. Q. Lin and G. P. Agrawal, "Vector Theory of Four-wave Mixing: Polarization Effects in Fiber-optic Parametric Amplifiers," J. Opt. Soc. Am. B **21**(6), 1216–1224 (2004).
34. G.-W. Lu, T. Sakamoto, and T. Kawanishi, "Wavelength Conversion of Optical 64QAM through FWM in HNLF and its Performance Optimization by Constellation Monitoring," Opt. Express **22**(1), 15–22 (2014).
35. K. Bottrill, N. Taengnoi, F. Parmigiani, D. Richardson, and P. Petropoulos, "Dataset for 'PAM4 transmission over 360 km of fibre using optical phase conjugation'," University of Southampton, accessed 3 Jan 2019.